Optical-constants model for semiconductors and insulators

Y. F. Chen and C. M. Kwei
Department of Electronics Engineering, National Chiao Tung University, Hsinchu, Taiwan, Republic of China

C. J. Tung*
Institute of Nuclear Science, National Tsing Hua University, Hsinchu, Taiwan, Republic of China
(Received 5 April 1993)

The refractive index and the extinction coefficient, i.e., the real and imaginary parts of the complex index of refraction, for semiconductors and insulators are derived as a function of photon energy. These derivations apply f-sum rules and symmetry relations to critical-point transitions from the valence band to the conduction band. Comparison with measured optical data reveals that present formulations are valid over a wide range of photon energies immediately above the band gap to the first ionization threshold for inner shells. The present work shows an improvement and extension over the theory of Forouhi and Bloomer, which applies for a narrow range of photon energies above the absorption edge.

I. INTRODUCTION

Optical properties of solids can be characterized by quantities such as the complex index of refraction $n(\omega)=\eta(\omega)+i\kappa(\omega)$ and the complex dielectric function $\varepsilon(\omega)=\varepsilon_1(\omega)+i\varepsilon_2(\omega)$. These quantities are photon energy ω dependent and provide information on the propagation of radiation and on the electronic structure of solids.[1,2] Optical quantities are useful in the design of mirrors, prisms, multilayers, etc.

The refractive index $\eta(\omega)$ and the extinction coefficient $\kappa(\omega)$ are commonly determined by reflective and absorptive spectroscopies.[3-6] Utilizing modern synchrotron radiation sources, these quantities can be measured over a wide range of photon energies, from the far infrared to the hard x-ray region. Theoretical formulations of η and κ can be obtained by the energy-dependent dielectric function through the relations $\eta=\{[(\varepsilon_1^2+\varepsilon_2^2)^{1/2}+\varepsilon_1]/2\}^{1/2}$ and $\kappa=\{[(\varepsilon_1^2+\varepsilon_2^2)^{1/2}-\varepsilon_1]/2\}^{1/2}$. The real and imaginary parts of the dielectric function, ε_1 and ε_2, can be derived by the quantum theory for the interaction between radiation and matter.[7] A widely accepted model for the derivation of dielectric functions is the extended Drude model[8,9] for the description of collective oscillations and interband transitions. Parameters in this model are determined by a fit of the imaginary part of the dielectric function to corresponding experimental data.

However, it is the refractive index and the extinction coefficient rather than the dielectric function which are experimentally accessible. Therefore, analytical expressions for the former two quantities are useful in the determination of fitting parameters and in the analysis of experimental data. Previously, such expressions for semiconductors and insulators were established[10-13] only for a narrow range of photon energies immediately above the band gap. Later, Forouhi and Bloomer (FB) (Refs. 14 and 15) derived a formula for the extinction coefficient to extend the validity to photon energies in the vicinity of interband transitions. The FB formula suffers at least two deficiencies, i.e., the extinction coefficient does not satisfy the symmetry relation and it does not comply with f-sum rules. As a consequence, their formula cannot be applied to photon energies around and above the plasmon resonant energies.

In the present work, we construct an analytical expression for the extinction coefficient which satisfies the symmetry relation and sum rules. We also derive an expression for the refractive index by applying Kramers-Kronig dispersion relations. These expressions are then applied to the critical-point transitions for electrons from the valence band to the conduction band of insulators and semiconductors. Comparing the results between this work and experimental data on $\eta(\omega)$, $\kappa(\omega)$, $\varepsilon_1(\omega)$, $\varepsilon_2(\omega)$, and the energy-loss function $\mathrm{Im}[-1/\varepsilon(\omega)]$, it is demonstrated that present formulas for the optical quantities are valid for photon energies over a wide range from the band gap to the edge of inner shells.

II. THEORY

A. f-sum rules

f-sum rules are important constraints for the analysis of energy-dependent optical quantities. These rules may be expressed in different forms involving the imaginary part of the dielectric function, $\varepsilon_2(\omega)$, the extinction coefficient $\kappa(\omega)$, and the energy-loss function $\mathrm{Im}[-1/\varepsilon(\omega)]$. They are explicitly expressed as[16]

$$\int_0^\infty \omega'\varepsilon_2(\omega')d\omega'=\frac{\pi}{2}\omega_p^2 , \tag{1}$$

$$\int_0^\infty \omega'\kappa(\omega')d\omega'=\frac{\pi}{4}\omega_p^2 , \tag{2}$$

and

$$\int_0^\infty \omega'\mathrm{Im}\left[\frac{-1}{\varepsilon(\omega')}\right]d\omega'=\frac{\pi}{2}\omega_p^2 , \tag{3}$$

where $\omega_p=\hbar(4\pi NZe^2/m)^{1/2}$ is the free-electron plasma energy, N is the atomic (or molecular) density, Z is the

total number of electrons per atom (or molecule), and e and m are, respectively, electron charge and mass. Note that these sum rules apply to optical quantities contributed by all absorption processes including valence-band excitations and inner-shell ionizations over the entire energy interval: $\omega=0\rightarrow\infty$.

A typical spectrum of the optical quantity usually reveals well-separated peaks, with little overlapping, due to different absorption processes. In such a case, one can set the upper limit of integration in Eqs. (1)–(3) equal to an energy cutoff $\tilde{\omega}_i$, large compared to the ith peak energy but small compared to other peak energies. Thus the above sum rules may be separated into individual contribution from each isolated absorption process by the approximate relations

$$\int_0^{\tilde{\omega}_i}\omega'\varepsilon_2(\omega')d\omega'\approx\frac{\pi}{2}\omega_{p,i}^2 , \tag{4}$$

$$\int_0^{\tilde{\omega}_i}\omega'\kappa(\omega')d\omega'\approx\frac{\pi}{4}\frac{\omega_{p,i}^2}{\eta_b} , \tag{5}$$

and

$$\int_0^{\tilde{\omega}_i}\omega'\mathrm{Im}\left[\frac{-1}{\varepsilon(\omega')}\right]d\omega'\approx\frac{\pi}{2}\frac{\omega_{p,i}^2}{\eta_b^4} , \tag{6}$$

where $\omega_{p,i}$ is the plasmon energy associated with the ith absorption process and η_b is the background refractive index. Note that the above partial f-sum rules for $\kappa(\omega)$ and $\mathrm{Im}[-1/\varepsilon(\omega)]$ yield effective oscillator strengths that are reduced by η_b and η_b^4 due to the shielding of other absorption processes. A detailed discussion about the background refractive index will be given below.

It is useful to define an effective number of electrons per atom (or molecule) corresponding to a given optical quantity according to

$$n_{\mathrm{eff}}(\omega)\Big|_{\varepsilon_2}=\frac{m}{2\pi^2e^4\hbar^2N}\int_0^{\omega}\omega'\varepsilon_2(\omega')d\omega' , \tag{7}$$

$$n_{\mathrm{eff}}(\omega)\Big|_{\kappa}=\frac{m}{\pi^2e^4\hbar^2N}\int_0^{\omega}\omega'\kappa(\omega')d\omega' , \tag{8}$$

and

$$n_{\mathrm{eff}}(\omega)\Big|_{\varepsilon^{-1}}=\frac{m}{2\pi^2e^4\hbar^2N}\int_0^{\omega}\omega'\mathrm{Im}\left[\frac{-1}{\varepsilon(\omega')}\right]d\omega' . \tag{9}$$

For each absorption process, we expect that

$$n_{\mathrm{eff}}(\omega)|_{\varepsilon_2}:n_{\mathrm{eff}}(\omega)|_{\kappa}:n_{\mathrm{eff}}(\omega)|_{\varepsilon^{-1}}\approx 1:\eta_b^{-1}:\eta_b^{-4}$$

in the limit $\omega\rightarrow\tilde{\omega}_i$. Equations (7)–(9) provide guidance for the determination of the number of valence electrons participating in critical-point transitions.

B. Index of refraction

Consider the forward propagation of photons in a solid.[17] The first-order time-dependent perturbation theory under the electric dipole approximation gives[15]

$$W(\omega)=\frac{4\pi^2e^2\omega I}{3\hbar c}|\langle\mathbf{k}_{\mathrm{crit}}^c|\mathbf{x}|\mathbf{k}_{\mathrm{crit}}^v\rangle|^2\delta(\omega-\omega_0) , \tag{10}$$

where $W(\omega)$ is the energy absorbed by the solid in the range ω to $\omega+d\omega$ per unit time, I is the incident photon intensity, c is the speed of light, and the Dirac δ function is owing to the conservation of energy. For the moment, we consider a single critical-point transition from the valence band to the conduction band, with transition matrix element $\langle\mathbf{k}_{\mathrm{crit}}^c|\mathbf{x}|\mathbf{k}_{\mathrm{crit}}^v\rangle$ and the transition energy $\omega_0=E_c-E_v$. The extinction coefficient is given by

$$\kappa(\omega)=\frac{\hbar c\rho(\omega)W(\omega)}{2\omega I} , \tag{11}$$

where $\rho(\omega)$ is the number of possible transitions in the range ω to $\omega+d\omega$ per unit volume. Defining the dipole oscillator strength of the transition as

$$f_0=\frac{8\pi e^2\omega_0}{3}|\langle\mathbf{k}_{\mathrm{crit}}^c|\mathbf{x}|\mathbf{k}_{\mathrm{crit}}^v\rangle|^2\rho(\omega_0) , \tag{12}$$

and substituting it into Eqs. (10) and (11), we obtain

$$\kappa(\omega)=\frac{\pi f_0}{4\omega_0}\delta(\omega-\omega_0) . \tag{13}$$

Equation (13) does not satisfy the symmetry relation,[18] i.e., $\kappa(\omega)=-\kappa(-\omega)$. To rectify this situation, we let

$$\kappa(\omega)=\frac{\pi f_0}{4\omega_0}[\delta(\omega-\omega_0)-\delta(\omega+\omega_0)] . \tag{14}$$

The extinction coefficient of Eq. (14) also satisfies the sum rule of Eq. (2). In this case, however, the lower limit of integration must be extended from 0 to $-\infty$ with the right-hand side of this equation multiplying by 2. Derivations so far assume zero energy breadth or infinite lifetime for the excited state in the critical-point transition. This assumption leads to the δ-function dependence of the extinction coefficient on photon energy. In reality, the spontaneous emission produces the damping of excited states.[7] To accommodate the damping effect, one may replace the δ functions in Eq. (14) by the Lorentzian line-shape function according to

$$\delta(\omega\pm\omega_0)\rightarrow\frac{1}{\pi}\frac{\Gamma_0}{(\omega\pm\omega_0)^2+\Gamma_0^2} , \tag{15}$$

where Γ_0 is the damping parameter relating to the full width at half maximum of the $\kappa(\omega)$ spectrum. Therefore, the extinction coefficient becomes

$$\kappa(\omega)=\frac{f_0\Gamma_0\omega}{[(\omega-\omega_0)^2+\Gamma_0^2][(\omega+\omega_0)^2+\Gamma_0^2]} . \tag{16}$$

The refractive index is connected to the extinction coefficient by Kramers-Kronig (KK) dispersion relations. These relations are direct consequences of the causality principle. Based on the Hilbert transform in KK relations, it gives[18]

$$\eta(\omega)=\eta_b+\frac{1}{\pi}\mathrm{P}\int_{-\infty}^{\infty}\frac{\kappa(\omega')}{\omega'-\omega}d\omega' , \tag{17}$$

where P denotes the Cauchy's principal value. Substitut-

ing Eq. (16) into Eq. (17), we obtain

$$\eta(\omega)=\eta_b-\frac{1}{2}\frac{f_0(\omega^2-\omega_0^2-\Gamma_0^2)}{[(\omega-\omega_0)^2+\Gamma_0^2][(\omega+\omega_0)^2+\Gamma_0^2]} . \quad (18)$$

The above formulas for the refractive index and the extinction coefficient are approximate since they are derived by first neglecting the damping effect and then resuming this effect using a Lorentzian line-shape function. Corresponding approximate formulas for the real and imaginary parts of the dielectric function can also be derived using Eqs. (16) and (18) and the relations $\varepsilon_1(\omega)=\eta^2(\omega)-\kappa^2(\omega)$ and $\varepsilon_2(\omega)=2\eta(\omega)\kappa(\omega)$. Alternatively, the quantum theory yields a Drude-type dielectric function as[8,9]

$$\varepsilon_1(\omega)=\varepsilon_b-\frac{F_0(\omega^2-\omega_0^2)}{(\omega^2-\omega_0^2)^2+\omega^2\gamma_0^2} \quad (19)$$

and

$$\varepsilon_2(\omega)=\frac{F_0\gamma_0\omega}{(\omega^2-\omega_0^2)^2+\omega^2\gamma_0^2} , \quad (20)$$

where ε_b is the background dielectric function of the solid, F_0 is related to the oscillator strength, and γ_0 is the damping parameter. Comparing the approximate dielectric function with the Drude dielectric function, we find that they are equal under conditions $\varepsilon_b=\eta_b^2$, $F_0=f_0\eta_b$, $\gamma_0=2\Gamma_0$, $\Gamma_0\ll\omega_0$, and $f_0\ll\omega_0^2$. To illustrate this comparison, in Fig. 1 we plot results in $\varepsilon_1(\omega)$, $\varepsilon_2(\omega)$, and $\mathrm{Im}[-1/\varepsilon(\omega)]$ calculated using the approximate (solid curves) and the Drude (dashed curves) formulas under conditions $\varepsilon_b=\eta_b=1$, $\Gamma_0=\omega_0/10$, and $f_0=\omega_0^2/10$. It is seen that fairly good agreement is found for all functions plotted. The imposed conditions $\Gamma_0\ll\omega_0$ and $f_0\ll\omega_0^2$ make Eqs. (16) and (18) valid only for insulators and semiconductors where ω_0 are large enough to satisfy these conditions.

The above formulations are for a single critical-point transition of electrons from the valence to the conduction bands. The generalization of these formulations to a general situation for several critical-point transitions can be made in a straightforward way. It is not difficult to show that each critical-point transition makes an independent contribution to the extinction coefficient. Thus, one can divide the oscillator strength into fractions f_i with transition energy ω_i and damping coefficient Γ_i. Let

$$f_i=\frac{8\pi e^2\omega_i}{3}|\langle \mathbf{k}^c_{\mathrm{crit}}|\mathbf{x}|\mathbf{k}^v_{\mathrm{crit}}\rangle_i|^2\rho(\omega_i) \quad (21)$$

be the oscillator strength for the ith critical-point transition. One can generalize Eqs. (16) and (18) into

$$\kappa(\omega)=\sum_{i=1}^{q}\frac{f_i\Gamma_i\omega}{[(\omega-\omega_i)^2+\Gamma_i^2][(\omega+\omega_i)^2+\Gamma_i^2]} \quad (22)$$

and

$$\eta(\omega)=\eta_b-\tfrac{1}{2}\sum_{i=1}^{q}\frac{f_i(\omega^2-\omega_i^2-\Gamma_i^2)}{[(\omega-\omega_i)^2+\Gamma_i^2][(\omega+\omega_i)^2+\Gamma_i^2]} , \quad (23)$$

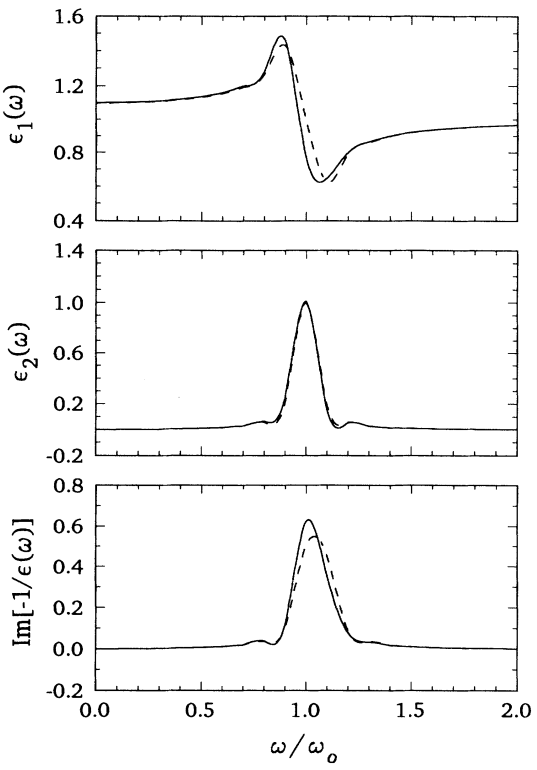

FIG. 1. A plot of $\varepsilon_1(\omega)$, $\varepsilon_2(\omega)$, and $\mathrm{Im}[-1/\varepsilon(\omega)]$ calculated using Eqs. (16) and (18) and the relations $\varepsilon_1=\eta^2-\kappa^2$ and $\varepsilon_2=2\eta\kappa$ (solid curves) and using Eqs. (19) and (20) (dashed curves) by taking $\varepsilon_b=\eta_b=1$, $\Gamma_0=\omega_0/10$, and $f_0=\omega_0^2/10$.

where q is the total number of critical-point transitions from the valence to the conduction bands.

To show that η_b is indeed the background refractive index due to the contribution from core electrons in inner shells, one can rewrite Eq. (23) as

$$\eta(\omega)=1-\tfrac{1}{2}\sum_{i=1}^{q}\frac{f_i(\omega^2-\omega_i^2-\Gamma_i^2)}{[(\omega-\omega_i)^2+\Gamma_i^2][(\omega+\omega_i)^2+\Gamma_i^2]} -\tfrac{1}{2}\sum_{j=1}^{c}\frac{f_j(\omega^2-\omega_j^2-\Gamma_j^2)}{[(\omega-\omega_j)^2+\Gamma_j^2][(\omega+\omega_j)^2+\Gamma_j^2]} , \quad (24)$$

where the first and second summation terms indicate, respectively, contributions from the valence band (having q critical-point transitions) and from inner shells (with c excitation groups). Since we are interested in the energy region $\omega\ll\omega_j$ ($j=1$ to c), Eq. (24) reduces to Eq. (23) with

$$\eta_b\approx 1+\tfrac{1}{2}\sum_{j=1}^{c}\frac{f_j}{\omega_j^2+\Gamma_j^2} . \quad (25)$$

It is seen that core electrons contribute to the background refractive index by an amount directly proportional to their oscillator strengths but inversely proportional to the square binding energies. Equation (25) will be applied to a few examples discussed below.

III. RESULTS AND DISCUSSION

We now fit Eq. (22) to optical data[19–23] for several insulators and semiconductors. Tables I–IV list the fitting parameters for MgO, SiO_2, Si, and GaAs. In these fittings, we check the accuracy of optical quantities including η, κ, and $\mathrm{Im}(-1/\varepsilon)$, critical-point energies ω_i, and sum rules of Eqs. (4)–(6) by comparing fitted values to experimental data. It is confirmed that the total oscillator strength of critical-point transitions satisfies the sum rule, i.e., $\sum_{i=1}^{q} f_i = \omega_{p,v}^2/\eta_b$, with $\omega_{p,v}$ being the plasmon energy of valence electrons. Critical-point energies measured by the optical reflectometry[24,25] and calculated by the pseudopotential band theory[26] for Si and GaAs are also listed in Tables III and IV for comparison. For MgO and SiO_2, our fits extend to $\omega = 300$ eV, which exceeds the L-shell threshold energies of Mg and Si. In these cases, the first eleven terms ($i = 1-11$) in Tables I and II correspond to critical-point transitions of the valence band, whereas the last three terms ($i = 12, 13, 14$) are associated with L-shell excitations of Mg and Si. Neglecting the K-shell contribution, we find that the refractive index at the region well below the L-shell excitation energy may be given by Eq. (24) with 14 terms or by Eq. (23) with 11 terms. In the latter equation we find that $\eta_b = 1.035$ and 1.004 for MgO and SiO_2, respectively. Thus the background refractive index is indeed determined by Eq. (25).

Figure 2 shows a comparison of $\eta(\omega)$, $\kappa(\omega)$, and $\mathrm{Im}[-1/\varepsilon(\omega)]$ for semiconducting Si calculated presently (solid curves) using Eqs. (22) and (23) and the relations $\varepsilon_1 = \eta^2 - \kappa^2$ and $\varepsilon_2 = 2\eta\kappa$, measured experimentally (dashed curves) and determined by FB (chain curves). It is seen that close agreement is found between present results and experimental data for all quantities plotted. It is also seen that prominent interband transitions, represented by the strong resonant peaks in η and κ spectra, occur in the region of critical-point energies below ~ 10 eV. Above this energy, the refractive index gradually approaches the asymptotic value η_b, and the extinction coefficient decreases with ω^{-3}. The corresponding FB re-

TABLE I. Parameters in Eqs. (22) and (23) for MgO.

	$\eta_b = 1$ (1.035 if $i = 1$ to 11 are used)		
i	f_i (eV^2)	Γ_i (eV)	ω_i (eV)
1	2	0.10	7.8
2	24	1.30	9.1
3	35	0.90	11.0
4	35	0.59	13.3
5	24	0.91	14.8
6	84	1.40	17.5
7	38	1.00	19.4
8	28	0.79	21.2
9	29	1.58	24.1
10	131	7.47	34.0
11	143	11.92	49.0
12	18	1.96	58.0
13	95	8.95	72.0
14	500	29.64	99.0

TABLE II. Parameters in Eqs. (22) and (23) for SiO_2.

	$\eta_b = 1$ (1.004 if $i = 1$ to 11 are used)		
i	f_i (eV^2)	Γ_i (eV)	ω_i (eV)
1	6	0.16	10.2
2	15	0.60	11.6
3	10	0.69	12.4
4	38	1.31	14.0
5	51	1.70	16.9
6	110	3.96	20.0
7	45	4.97	25.0
8	41	5.00	30.0
9	33	4.98	40.0
10	70	8.00	51.0
11	63	12.94	72.0
12	16	5.95	108.0
13	58	14.90	134.6
14	170	59.82	189.5

TABLE III. Parameters in Eqs. (22) and (23) for Si.

	$\eta_b = 1.015$			Experimental reflectivity	Theoretical critical-point
i	f_i (eV^2)	Γ_i (eV)	ω_i (eV)	structure (eV)	analysis (eV)
1	0.2	0.01	3.43	3.40	3.42
2	0.4	0.01	3.48	3.45	3.48
3	11.0	0.36	3.72	3.66	
4	16.0	0.25	4.35	4.30	4.47
5	10.0	0.30	4.75	4.57	4.60
6	21.0	0.50	5.45	5.48	5.56
7	23.0	0.70	6.40		
8	70.0	1.60	7.80		
9	70.0	2.30	10.60		
10	50.0	2.80	14.00		

TABLE IV. Parameters in Eqs. (22) and (23) for GaAs.

	$\eta_b = 1.01$			Experimental reflectivity	Theoretical critical-point
i	f_i (eV^2)	Γ_i (eV)	ω_i (eV)	structure (eV)	analysis (eV)
1	0.8	0.10	3.03	3.02	3.03
2	3.4	0.20	3.25	3.25	3.25
3	5.8	0.40	3.70		
4	13.0	0.50	4.60	4.64	4.54
5	20.0	0.40	5.05	5.11	5.07
6	13.0	0.50	5.76	5.64	5.76
7	20.0	0.79	6.70	6.60	6.67
8	44.0	1.40	8.00		
9	59.0	2.20	10.50		9.87
10	49.0	2.20	13.50		12.55
11	13.0	1.70	21.50		

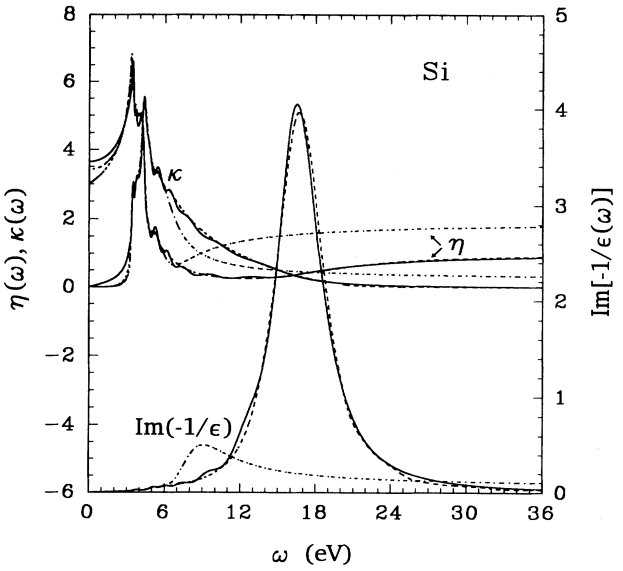

FIG. 2. A comparison of $\eta(\omega)$, $\kappa(\omega)$, and $\mathrm{Im}[-1/\varepsilon(\omega)]$ for Si calculated using Eqs. (22) and (23) and the relations $\varepsilon_1=\eta^2-\kappa^2$ and $\varepsilon_2=2\eta\kappa$ (solid curves), measured experimentally (dashed curves) (Ref. 21) and determined by FB (chain curves) (Ref. 15).

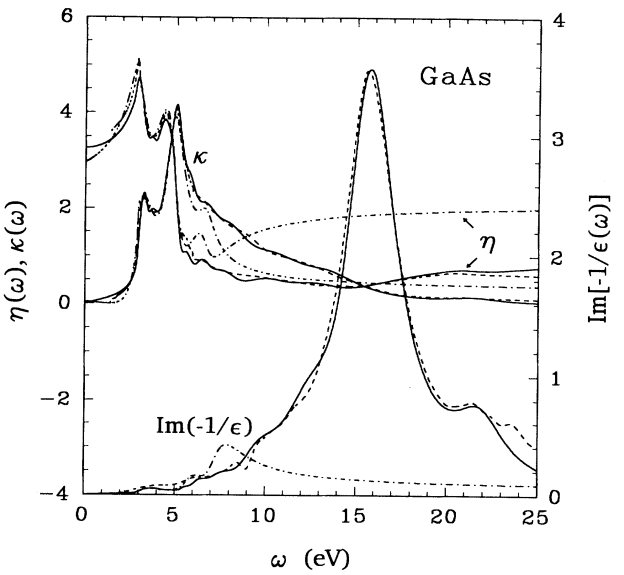

FIG. 4. A comparison of $\eta(\omega)$, $\kappa(\omega)$, and $\mathrm{Im}[-1/\varepsilon(\omega)]$ for GaAs calculated using Eqs. (22) and (23) and the relations $\varepsilon_1=\eta^2-\kappa^2$ and $\varepsilon_2=2\eta\kappa$ (solid curves), measured experimentally (dashed curves) (Refs. 22 and 23) and determined by FB (chain curves) (Ref. 15).

sults, on the other hand, approach constant values for both optical quantities. The constant value of the FB extinction coefficient at large ω is clearly incorrect because the integral in the sum rule of Eq. (2) will then diverge. Comparing with the experimental data, it is indicated that the validity of FB results is restricted to photon energies below ~ 7 eV. This is true especially for the energy-loss function, where FB results are totally invalid above that energy. Figure 3 shows a plot of $n_{\mathrm{eff}}(\omega)$, defined in Eqs. (7)–(9), for Si calculated presently (solid curves), measured experimentally (dashed curves), and determined using FB optical quantities (chain curves). It is seen that the effective number of valence electrons per atom saturates to four valence electrons at $\omega=80$ eV, with the modification according to $n_{\mathrm{eff}}(\omega)|_{\varepsilon_2}:n_{\mathrm{eff}}(\omega)|_{\kappa}:n_{\mathrm{eff}}(\omega)|_{\varepsilon^{-1}}\approx 1:\eta_b^{-1}:\eta_b^{-4}$. It is also seen that FB formulas lead to unphysical results for $n_{\mathrm{eff}}(\omega)|_{\kappa}$

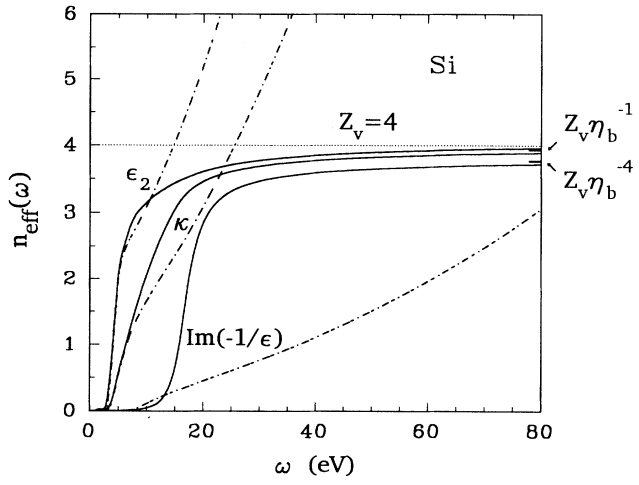

FIG. 3. The results of $n_{\mathrm{eff}}(\omega)|_{\varepsilon_2}$, $n_{\mathrm{eff}}(\omega)|_{\kappa}$, and $n_{\mathrm{eff}}(\omega)|_{\varepsilon^{-1}}$ for Si calculated presently (solid curves), using experimental data (dashed curves) (Ref. 21) and using FB optical quantities (chain curves) (Ref. 15). The dotted line at $Z_v=4$ represents the saturation value for the number of valence electrons per atom.

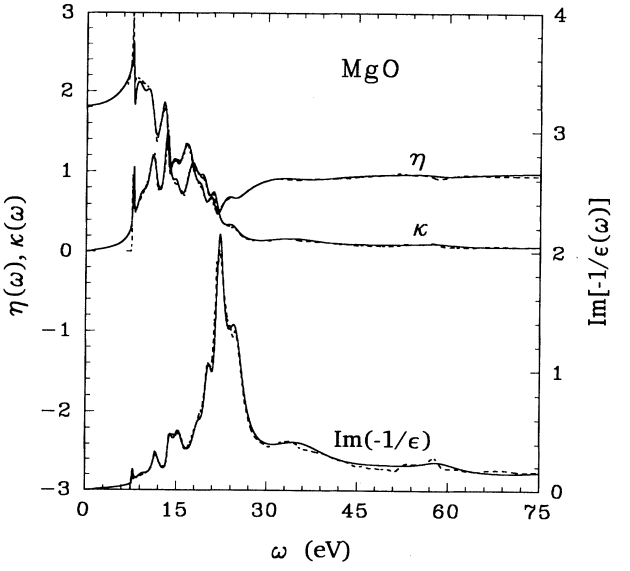

FIG. 5. A comparison of $\eta(\omega)$, $\kappa(\omega)$, and $\mathrm{Im}[-1/\varepsilon(\omega)]$ for MgO calculated using Eqs. (22) and (23) and the relations $\varepsilon_1=\eta^2-\kappa^2$ and $\varepsilon_2=2\eta\kappa$ (solid curves) and measured experimentally (dashed curves) (Ref. 19).

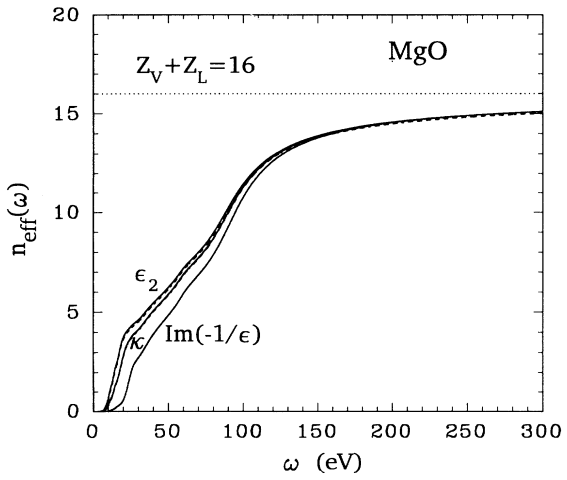

FIG. 6. The results of $n_{\text{eff}}(\omega)|_{\varepsilon_2}$, $n_{\text{eff}}(\omega)|_{\kappa}$, and $n_{\text{eff}}(\omega)|_{\varepsilon^{-1}}$ for MgO calculated presently (solid curves) and using experimental data (dashed curves) (Ref. 19). The dotted line at $Z_V+Z_L=16$ represents the saturation value for the number of electrons contributing to an isolated absorpting group.

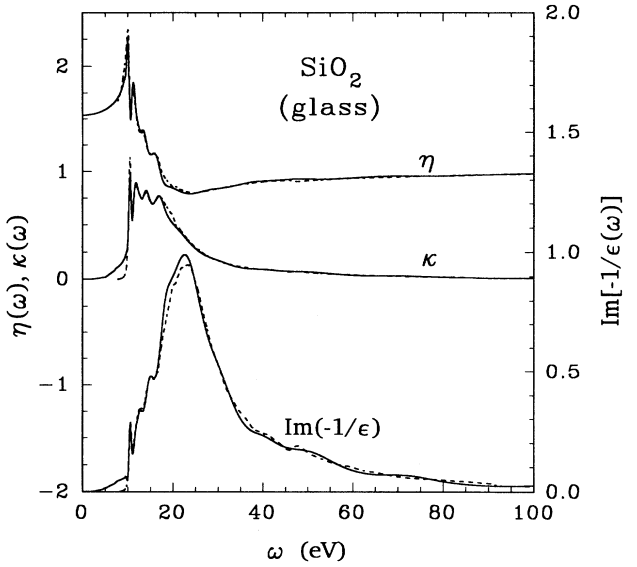

FIG. 7. A comparison of $\eta(\omega)$, $\kappa(\omega)$, and Im$[-1/\varepsilon(\omega)]$ for SiO_2 glass calculated using Eqs. (22) and (23) and the relations $\varepsilon_1=\eta^2-\kappa^2$ and $\varepsilon_2=2\eta\kappa$ (solid curves) and measured experimentally (dashed curves) (Ref. 20).

and $n_{\text{eff}}(\omega)|_{\varepsilon_2}$ at large ω. The FB results on $n_{\text{eff}}(\omega)|_{\varepsilon^{-1}}$ also deviate greatly compared to experimental data at $\omega>15$ eV.

Similarly, in Fig. 4 we plot the results of $\eta(\omega)$, $\kappa(\omega)$, and Im$[-1/\varepsilon(\omega)]$ for semiconducting GaAs calculated presently (solid curves), measured experimentally (dashed curves), and determined by FB (chain curves). It is again seen that close agreement is found between present results and experimental data for all quantities plotted. The small deviations occurring at $\omega>22$ eV are due to the contribution from d-band excitations. The onset of these excitations is $\sim$25 eV, above which optical data are unavailable. It is also seen that the FB results are in agreement with experimental data only for $\omega<6$ eV. The failure of these results around and above plasmon energies is clearly demonstrated.

As an example of insulators, in Fig. 5 we plot $\eta(\omega)$, $\kappa(\omega)$, and Im$[-1/\varepsilon(\omega)]$ for MgO. Here the agreement between present results (solid curves) and experimental data (dashed curves) is quite good for all quantities plotted. Figure 6 shows a plot of $n_{\text{eff}}(\omega)$ calculated presently (solid curves) and measured experimentally (dashed curves) for MgO. Note that the saturation value of $n_{\text{eff}}(\omega)|_{\varepsilon_2}$ is near 16 instead of 8, the number of valence electrons. This is due to the onset of Mg L-shell excitations near 55 eV; there only about 75% of the oscillator strength of valence electrons is exhausted. Thus a strong overlapping of oscillator strengths between the valence band and the Mg L shell exists above 55 eV. Also, the next filled O K shell lies $\sim$500 eV above the valence band. Therefore, the isolated absorption group should include eight valence electrons ($3s^2$ of Mg; $2s^2$ and $2p^4$ of O) and eight Mg L-shell electrons ($2s^2$ and $2p^6$ of Mg). The merge of saturation values of all three $n_{\text{eff}}(\omega)$ spectra indicates that $\eta_b\approx 1$. It means that absorption peaks of Mg and O K shells are far away from critical-point transition peaks of the valence band.

Finally, in Fig. 7 we plot optical quantities for another insulator, SiO_2 glass. Good agreement is found between present results (solid curves) and experimental data (dashed curves). In this case, the isolated absorption group involves 16 valence electrons ($3s^2$ and $3p^2$ of Si; $2s^2$ and $2p^4$ of O) and 8 Si L-shell electrons ($2s^2$ and $2p^6$ of Si). The saturation of $n_{\text{eff}}(\omega)$ to 24 occurs at $\omega\approx 300$ eV.

IV. CONCLUSIONS

We have constructed analytical expressions for the extinction coefficient and the refractive index of semiconductors and insulators. Our approach involved the application of f-sum rules and symmetry relations. These expressions contain parameters characterizing the oscillator strength, the damping effect, and the transition energy associated with each critical-point transition from the valence to the conduction bands. Contributions from inner shells to the refractive index in the vicinity of critical-point energies were included as a background refractive index. Applications of present formulations were made for MgO, SiO_2, Si, and GaAs over a wide range of photon energies. Results were in very good agreement with experimental data for all optical quantities studied.

ACKNOWLEDGMENT

This work was supported by the National Science Council of the Republic of China under Contract No. NSC82-0208-M-009-013.

*Present address: Department of Nuclear Engineering, Texas A&M University, College Station, TX 77843.

[1]F. Bassani and G. P. Parravicini, *Electronic States and Optical Transitions in Solids* (Pergamon, Oxford, 1975).
[2]F. Wooten, *Optical Properties of Solids* (Academic, New York, 1972).
[3]R. M. A. Azzam and N. M. Bashara, *Ellipsometry and Polarized Light* (North-Holland, Amsterdam, 1977).
[4]P. S. Hauge, Surf. Sci. **96**, 108 (1979).
[5]R. H. Muller, Surf. Sci. **56**, 19 (1976).
[6]A. V. Rzhanov and K. K. Svitashev, Adv. Electron. Electron Phys. **49**, 1 (1979).
[7]R. Loudon, *The Quantum Theory of Light* (Clarendon, Oxford, 1973).
[8]H. Raether, *Excitations of Plasmons and Interband Transitions by Electrons,* Springer Tracts in Modern Physics Vol. 88 (Springer, Berlin, 1980).
[9]C. M. Kwei, T. L. Lin, and C. J. Tung, J. Phys. B **21**, 2901 (1988); see also C. M. Kwei, Y. F. Chen, C. J. Tung, and J. P. Wang, Surf. Sci. (to be published).
[10]D. L. Greenaway and G. Harbeke, *Optical Properties and Band Structure of Semiconductors* (Pergamon, Oxford, 1968).
[11]J. I. Pankove, *Optical Processes in Semiconductors* (Dover, New York, 1971).
[12]J. C. Phillips, *Bonds and Bands in Semiconductors* (Academic, New York, 1973).
[13]*Handbook of Optical Constants of Solids,* edited by E. D. Palik (Academic, New York, 1985).
[14]A. R. Forouhi and I. Bloomer, Phys. Rev. B **34**, 7018 (1986).
[15]A. R. Forouhi and I. Bloomer, Phys. Rev. B **38**, 1865 (1988).
[16]D. Y. Smith and E. Shiles, Phys. Rev. B **17**, 4689 (1978).
[17]J. J. Sakurai, *Advanced Quantum Mechanics* (Addison-Wesley, Reading, MA, 1967).
[18]H. M. Nussenzveig, *Causality and Dispersion Relations* (Academic, New York, 1972).
[19]D. M. Roessler and D. R. Huffman, in *Handbook of Optical Constants of Solids II,* edited by E. D. Palik (Academic, New York, 1991), p. 919.
[20]H. R. Philipp, in *Handbook of Optical Constants of Solids I,* edited by E. D. Palik (Academic, New York, 1985), p. 749.
[21]D. F. Edwards, in *Handbook of Optical Constants of Solids I,* edited by E. D. Palik (Academic, New York, 1985), p. 547.
[22]D. E. Aspnes and A. A. Studna, Phys. Rev. B **27**, 985 (1983).
[23]C. V. Festenberg, Z. Phys. **227**, 453 (1969).
[24]R. R. L. Zucca, J. P. Walter, Y. R. Shen, and M. L. Cohen, Solid State Commun. **8**, 627 (1970).
[25]R. R. L. Zucca and Y. R. Shen, Phys. Rev. B **1**, 2668 (1970).
[26]J. R. Chelikowsky and M. L. Cohen, Phys. Rev. B **14**, 556 (1976).